Decision Tree Based Classification of Abdominal Aortic Aneurysms using Geometry Quantification Measures

Shalin A. Parikh[1], **Raymond Gomez**[2], **Mirunalini Thirugnanasambandam**[1], **Sathyajeeth S. Chauhan**[1], **Victor De Oliveira**[3], **Satish C. Muluk**[4], **Mark K. Eskandari**[5], and **Ender A. Finol**[1,2,*]

[1]University of Texas at San Antonio UTSA/UTHSA Joint Graduate Program in Biomedical Engineering One UTSA Circle San Antonio, TX 78249 U.S.A.

[2]University of Texas at San Antonio Department of Mechanical Engineering One UTSA Circle San Antonio, TX 78249 U.S.A.

[3]University of Texas at San Antonio Department of Management Science and Statistics One UTSA Circle San Antonio, TX 78249 U.S.A.

[4]Allegheny Health Network Allegheny General Hospital, Department of Thoracic & Cardiovascular Surgery 320 E. North Ave. Pittsburgh, PA 15212 U.S.A.

[5]Northwestern University Feinberg School of Medicine Division of Vascular Surgery and Department of Radiology 420 E. Superior St. Chicago, IL 60611 U.S.A.

Abstract

Abdominal aortic aneurysm (AAA) is an asymptomatic aortic disease with a survival rate of 20% after rupture. It is a vascular degenerative condition different from occlusive arterial diseases. The size of the aneurysm is the most important determining factor in its clinical management. However, other measures of the AAA geometry that are currently not used clinically may also influence its rupture risk. With this in mind, the objectives of this work are to develop an algorithm to calculate the AAA wall thickness and abdominal aortic diameter at planes orthogonal to the vessel centerline, and to quantify the effect of geometric indices derived from this algorithm on the overall classification accuracy of AAA based on whether they were electively or emergently repaired. Such quantification was performed based on a retrospective review of existing medical records of 150 AAA patients (75 electively repaired and 75 emergently repaired). Using an algorithm implemented within the MATLAB computing environment, 10 diameter- and wall thickness-related indices had a significant difference in their means when calculated relative to the AAA centerline compared to calculating them relative to the medial axis. Of these 10 indices, nine were wall thickness-related while the remaining one was the maximum diameter (D_{max}). D_{max} calculated with respect to the medial axis is over-estimated for both electively and emergently repaired AAA compared to its counterpart with respect to the centerline. C5.0 decision trees, a machine learning classification algorithm implemented in the R environment, were used to construct a statistical classifier. The decision trees were built by splitting the data into 70% for training and 30% for testing, and the properties of the classifier were estimated based on 1000 random combinations of the 70/30 data split. The ensuing model had average and maximum

*Corresponding author Tlf: (210) 458-8058, Fax: (210) 458-6504, ender.finol@utsa.edu.

classification accuracies of 81.0% and 95.6%, respectively, and revealed that the three most significant indices in classifying AAA are, in order of importance: AAA centerline length, L2-norm of the Gaussian curvature, and AAA wall surface area. Therefore, we infer that the aforementioned three geometric indices could be used in a clinical setting to assess the risk of AAA rupture by means of a decision tree classifier. This work provides support for calculating cross-sectional diameters and wall thicknesses relative to the AAA centerline and using size and surface curvature based indices in classification studies of AAA.

Keywords

aneurysm; geometric modeling; machine learning; decision trees

3.   INTRODUCTION

The overall mortality associated with the repair of ruptured abdominal aortic aneurysms (rAAA) is 30.7%, a composite of 33.4% of deaths occurring during open surgery and 26.2% of deaths during endovascular aneurysm repair (EVAR).[8] Currently, maximum diameter (> 5.5 cm) of an abdominal aortic aneurysm (AAA) and growth rate (> 1 cm/year) are used as clinical standards for recommending elective repair of the aneurysm. The basis for utilizing maximum diameter as a criterion may have originated from the Law of Laplace, which states that the circumferential stress in the aortic wall is directly proportional to its radius. This leads to larger aneurysms (i.e., with larger maximum diameters) having a higher wall stress that is believed to translate into a higher rupture risk.[22] However, since aneurysms have intricate geometries and varying radii of curvature, the Law of Laplace is unwarranted as it is only applicable for spherical or cylindrical geometries with thin walls (ratio of wall thickness to inner radius less than 0.1).[28] In addition, a study detailing autopsy results of 473 non-resected AAA indicated that 13% of AAA with a maximum diameter less than 5.5 cm ruptured while 60% of AAA with a maximum diameter greater than 5.5 cm never ruptured.[6] Of the latter, 54% had diameters ranging from 7.1 cm to 10 cm.[2] From these, we infer that the decision for recommending elective repair should not be solely based on the maximum diameter as small AAA with a high rupture risk would not be repaired in a timely manner. Likewise, there are avoidable interventions performed on AAA that are otherwise stable despite qualifying for elective repair based on their size. Vascular surgeons and interventional radiologists make a judgment on the need for repair by weighing the risks associated with an intervention versus the risk of aneurysm rupture. Results from four clinical trials (UKSAT, ADAM, PIVOTAL, and CAESAR) indicate that for small AAA, watchful waiting (i.e., monitoring at regular time intervals) is advised as survival chances are not improved by either open surgery or EVAR.[10] EVAR carries a mortality rate of < 2% while open abdominal surgery has a mortality rate of 2–4% and is far more invasive than EVAR, leading to greater co-morbidities.[12]

Geometry and biomechanics of AAA are known to be interdependent with variations in aneurysm geometries responsible for the spatial non-uniformity of wall stress distributions. Pappu and others[18] concluded from a study of 15 small AAA that three aneurysms that eventually ruptured had a 29% higher tortuosity than the average of the other 12 aneurysms.

This and other similar studies point to the convenience of defining a comprehensive set of geometric indices to quantify the AAA shape and surface curvature. To this end, the work of Martufi et al.[15] proposed the use of several one-dimensional, two-dimensional size and shape indices, and three-dimensional indices for quantifying patient specific AAA geometry. The indices can be used for individual rupture risk assessment by establishing thresholds based on a statistical classifier that uses numerous image datasets.[24] In a study by Tang et al.,[27] it was concluded that area-averaged Mean curvature (MAA) and bulge height (BL) were independently associated with AAA rupture risk. In their study, when these two indices were included in the rupture risk prediction model, the sensitivity and specificity of the model showed an increase of 4% and 2%, respectively. In a retrospective study of 76 aneurysms, Shum et al.[24] found that a classification algorithm based on maximum diameter (D_{max}), surface area (S), tortuosity (T), and ILT volume ratio ( ) had a classification accuracy of 86.6%.

Most image-based measurement methods use planes orthogonal to the medial (i.e. vertical) axis to quantify vessel diameter, leading to its over-estimation compared to using planes orthogonal to the centerline.[9] Therefore, quantifying geometric indices relative to the AAA centerline would be necessary to have a more reliable rupture risk classification model. Clinicians use the AAA centerline to estimate the maximum AAA diameter as the cross sections of the abdominal aorta may appear elliptical on medial planes due to projection, thus leading to low reproducibility of the estimates. Assessment of cross-sectional diameters is highly sensitive to whether the transverse planes are orthogonal to the centerline or to a prescribed medial axis.[7] Manning et al.[14] indicated that axial measures of diameter on computed tomography (CT) scans were higher than diameters measured orthogonal to the flow centerline of AAA by a mean of 2.4 5.0 mm.

Wall thickness has been known to affect mechanical wall stress and hence has the potential to be a rupture risk marker.[16] Di Martino and co-workers[3] found a substantial difference in wall thickness between ruptured (3.6 0.3 mm) and electively repaired (2.5 0.1 mm) AAA. Conversely, the work of Raghavan et al.[19] in an experimental study on one ruptured and three unruptured AAA indicates that there is a significant reduction in wall thickness near the rupture site (0.23 mm) in comparison to a calcified site (4.26 mm). Saccular aneurysms are more prone to rupture than fusiform aneurysms,[26] which supports the notion of shape-based indices as measures that can be used for rupture risk assessment. Peak wall stress increases non-linearly with AAA asymmetry,[19] which is a geometry index dependent on the aneurysm centerline. Similarly, Doyle et al.[4] studied 15 patient specific AAA and found an increase in wall stress of 38% with an increase in asymmetry. These studies substantiate the importance of asymmetry as a surrogate for wall stress.

In the present work, we perform a statistical comparison of geometric indices derived from local diameter and wall thickness measures calculated at planes orthogonal to the medial axis and orthogonal to the AAA centerline. In addition, we compute various other one-dimensional, two-dimensional and three-dimensional size and shape indices for a group of electively and emergently repaired AAA. We hypothesize that a set of geometric indices that includes aneurysm diameter and wall thickness measures calculated at planes orthogonal to the AAA centerline will yield the highest accuracy when discriminating between electively

and emergently repaired AAA. To this end, the contribution of this work is the construction of a statistical classifier based on geometry that can be used for rupture risk assessment in a clinical setting.

4. MATERIALS AND METHODS

A retrospective review of existing medical records was performed following approval of the human subjects research protocols by the corresponding Institutional Review Committees at Allegheny General Hospital (Pittsburgh, PA) and Northwestern Memorial Hospital (Chicago, IL). The abdominal computed tomography angiography (CTA) scans of 75 patients who underwent elective repair (Group 1 subjects) and 75 patients who underwent emergent repair of their AAA (Group 2 subjects) were obtained retrospectively from existing databases at the aforementioned clinical centers. The scans corresponded to the last available surveillance imaging, which occurred no greater than 1 month prior to the emergent intervention and no greater than 6 months prior to the elective repair. Noteworthy is that all Group 1 AAA were unruptured while Group 2 AAA included both ruptured and symptomatic AAA.

4.1 Image Processing

Using an in-house segmentation code (dubbed AAAVasc), computer models were generated for all patient specific AAA. Three anatomical regions were segmented, namely the lumen, inner wall and outer wall. The lumen segmentation algorithm quantifies the intensity gradient between the lumen and surrounding structures (wall or thrombus) and is primarily based on a thresholding technique.[25] The inner wall boundary is identified by training a neural network based on extracting the background, thrombus and lumen regions. This method gives an estimate of the region where the inner wall may be present. The outer wall is segmented by reducing the image region that only contains the aorta. Consequently, contours are identified that represent the aorta outer wall boundary and the best one is selected by the user. Additional details on the image processing protocol are described in [23]. Image processing yields point clouds for the lumen, inner wall and outer wall boundaries. In addition, binary masks are also created for the lumen, thrombus, wall, and background regions. These masks are used with an in-house meshing code (dubbed AAAMesh) to generate triangular outer wall surface and hexahedral+tetrahedral volume meshes for each AAA according to the methods described in [5, 20].

4.2 AAA Geometry Quantification Based on the Medial Axis

The CTA images are acquired at planes orthogonal to the Z-axis (i.e., the medial axis) and, thus, no additional processing is required to identify the planes orthogonal to this axis. Cubic splines are fit to the outer wall point clouds at each cross-section. From these, 47 shape- and size-based geometric indices were quantified for each AAA based on the mathematical formulations listed in Appendix A of the Supplementary Material. These include 11 (1-D) size indices, such as the length of the AAA centerline, height of the neck, distal and proximal neck diameters, etc., as shown in Figure 1. Nine (2-D) shape indices are calculated from the 1-D size indices, while 4 (3-D) size indices are calculated from the volumes enclosed by each domain using the volume meshes. Four (3-D) curvature-based shape

indices are quantified using the biquintic hermite finite element (BQFE) method, which is a high-order surface discretization method that requires only 12 elements to represent the AAA sac geometry.[7] Wall thickness is calculated based on 12 indices representative of various measures of thickness, as described in Appendix A of the Supplementary Material.

4.3   AAA Geometry Quantification Based on the Aneurysm Centerline

To calculate diameter and wall thickness at planes orthogonal to the AAA centerline, 3D planes are visualized at each cross-section centroid throughout the aneurysm sac. The Z-coordinate of each plane is calculated by solving Eq. (1),

$$\overrightarrow{n}(X - P1) + \overrightarrow{n}(Y - P1) + \overrightarrow{n}(Z - P1) = \overrightarrow{0} \quad (1)$$

where $\overrightarrow{n} = P2 - P1$, $P1$ and P_2 are consecutive points on the centerline, and x, Y and Z are the coordinates of the plane in the x, y and z axes, respectively.

Once the appropriate plane size is calculated, the inner wall points that lie on the plane are obtained using a k-nearest neighbors algorithm and the corresponding outer wall points are found as those closest to the inner wall points. Cubic splines are fit to the outer wall points and the area and perimeter of the spline are calculated after projecting it on the plane. As the AAA cross-sections are non-circular, the hydraulic diameter definition is used to calculate the diameters at each plane,[15] following Eq. (2),

$$Diameter = \frac{4A_c}{P_c} \quad (2)$$

where A_c is the area of cross-section and P_c is its perimeter. Wall thickness is defined as the shortest distance between an inner wall point and its corresponding outer wall point for all points on each orthogonal plane. The inner and outer wall points are interpolated leading to wall thicknesses calculated for approximately 300–400 points per crosssection. The wall thicknesses are used to compute 12 global wall thickness indices as described in Appendix A of the Supplementary Material. Four diameter-related indices are also calculated, namely maximum diameter (D_{max}), asymmetry ratio ( ), maximum diameter to proximal neck diameter ratio (DDr), and bulge height (BL). Therefore, 16 global wall thickness and diameter-related indices were calculated for each AAA with respect to the centerline of the AAA sac. A script written in MATLAB (The Mathworks Inc., Natick, MA) was generated to perform all the calculations involving the AAA centerline.

4.4   Statistical Analysis and Machine Learning

Using the methods described in Sections 4.2 and 4.3, all geometric indices were calculated for each of the 150 AAA. A series of paired t-tests were conducted to determine if the differences in the means of the 16 global diameter- and wall thicknessrelated indices obtained using the centerline and medial axis methods were significantly different. A p-value less than 0.05 was deemed to provide evidence of a statistically significant difference.

A machine learning analysis was carried out within the R environment, with the goal of deriving a geometry-based classifier for the AAA subject population. Specifically, the R package *C50* [11] was used to train decision trees to classify AAA as either electively or emergently repaired using the geometry-based measures as attributes. C5.0 decision trees depend on the concepts of information gain (IG) and entropy to determine the attributes that provide the highest information about the instances on which the tree is modeled. The IG is calculated for each of the attributes and the one with the smallest entropy (highest IG) forms the root node of the tree. The subsequent nodes are determined in the same way.[11] Some details regarding C5.0 decision trees can be found in Appendix B of the Supplementary Material. The area under the receiver operator characteristic (ROC) curve was computed for each of the models to determine the performance of the classifier. The kappa statistic () was also computed to provide a measure of accuracy of the decision tree classifier; it considers the instances identified correctly by chance in calculating the model accuracy and, thus, provides an additional measure of classification performance.

To evaluate the efficacy of the centerline based geometric indices on the overall AAA classification accuracy, four classification problems were analyzed:

(I) None of the 16 centerline based indices were used in training the model; thus, 16 of the 47 indices used in the model were calculated based on the medial axis. This model was used as a benchmark to make comparisons with the three classification problems that follow.

(II) Replacing the 4 diameter-related indices (D_{max}, *DDr*, and *BL*) of the model developed in (I) with their counterparts calculated based on the AAA centerline.

(III) Replacing the 12 global wall thickness indices of the model developed in (I) with their counterparts calculated based on the AAA centerline.

(IV) Replacing all 16 global wall thickness and diameter-related indices of the model developed in (I) with their counterparts calculated based on the AAA centerline.

The dataset was randomly split into 70% for training ($N_{training}$ = 105 AAA) and 30% for testing the models ($N_{testing}$ = 45 AAA) for each of the aforementioned classification problems. The rationale for performing a 70/30 split was to mimic the availability of a database of existing AAA from which a statistical classifier is trained and prospectively acquired AAA data on which the classifier is tested. The splitting was performed randomly for n = 1000 times, thus leading to 1000 different combinations of training and testing groups. The classification accuracy, the kappa statistic and area under the ROC curve (AUC) were averaged over all iterations. This was done to reduce the possibility of not considering a specific instance in training the model. Figure 2 shows a schematic of the study design workflow inclusive of the indices that are dependent on the choice of axis and the aforementioned four classification problems.

5. RESULTS

5.1 Comparison of Methods for Estimation of Cross-sectional Diameters and Wall Thicknesses

Paired t-tests were performed for all 16 diameter- and wall thickness-related indices to assess the significance of the mean differences found by using the two methods of calculation, namely with planes orthogonal to the medial axis and the AAA centerline. Table 1 shows the p-values obtained for these indices for Groups 1 and 2. The outcome of the tests for Group 1 indicate that the differences in the means were significant ($p < 0.05$) for the following 10 indices: D_{max}, average thickness, maximum thickness, minimum thickness, average wall thickness at D_{max}, mode thickness, mean thickness variance, median thickness variance, % thickness below average thickness, and % thickness above average thickness. Similarly, for Group 2, the differences in means for the following 9 indices were significant ($p < 0.05$): D_{max}, maximum thickness, minimum thickness, average wall thickness at D_{max}, mode thickness, median thickness, mean thickness variance, median thickness variance, and percent thickness above average thickness. Figure 3 illustrates histograms depicting the discrepancy in the means of maximum diameter and average wall thickness obtained by the two methods of calculation for both population groups and their statistical significance.

Table 2 shows the 31 geometric indices that are not dependent on the choice of planes orthogonal to either the medial axis or AAA centerline, reported as mean ± standard deviation, for the two groups of aneurysms. Additionally, Tables 3 and 4 report on the 16 diameter- and wall thickness-related indices for both groups calculated using planes orthogonal to the medial axis and AAA centerline, respectively. The mean D_{max} for Group 1 was 53.1 ± 11.4 mm when calculated with respect to the medial axis and 50.6 ± 11.8 mm when calculated with respect to the AAA centerline. Similarly, the mean average wall thickness for this group was 1.84 mm ± 0.55 mm when calculated with respect to the medial axis and 1.70 mm ± 0.50 mm when calculated with respect to the AAA centerline. For Group 2, the mean D_{max} was 68.8 ± 17.8 mm when calculated with respect to the medial axis and 64.6 ± 11.8 mm when calculated with respect to the AAA centerline. Likewise, the mean average wall thickness for Group 2 was 2.03 ± 0.60 mm and 1.85 mm ± 0.54 mm, calculated relative to each of the aforementioned methods, respectively.

5.2 Classification Based on Decision Tree Analysis

The average and maximum classification accuracies for the four classification problems using C5.0 decision trees, along with their kappa statistics and AUCs counterparts are shown in Table 5. These averages and maxima were calculated from the 1000 different decision tree models generated from the random splitting of the dataset into training and testing groups. For example, for problem (I) the average classification accuracy of the decision tree was 80.6% ± 6.0%, the average was 0.61 ± 0.12, and the average AUC was 0.81 ± 0.06. Over n = 1000 iterations, the decision tree model with the highest classification accuracy yielded a classification accuracy of 95.5%, = 0.91, and AUC = 0.96. Similar statistics are reported in Table 5 for classification problems (II) – (IV).

Figure 4 displays an exemplary decision tree model [for classification problem (I)], indicating the most significant geometric indices and their threshold values where each bifurcation takes place. L (AAA centerline length) is the first geometric index in the decision tree and, thus, the feature with the highest information gain. The other attributes (i.e. geometric indices) involved in the classifier are GLN, $t_{t,min}$, S, C_{ave}, DDr, and L_{sac}, and $t_{w,meanVar}$. The decision tree shown is based on the application of the classifier on all 150 AAA in the dataset. The correctly classified and misclassified instances are indicated at a particular node with the "/" sign and whether the instance corresponds to the electively repaired (Group 1) or emergently repaired (Group 2) AAA.

Table 6 shows the frequency of inclusion (in %) of the geometric indices as nodes of the trees for each classification problem. These are interpreted as a measure of relative importance of the geometric indices in the trees' ability to discriminate between Groups 1 and 2 aneurysms. The higher the percentage of inclusion, the more important the geometric index is in its ability to classify a given AAA as belonging to either group. For example, for classification problem (I), the AAA centerline length was used in 100% of the instances in which the classifier was applied to the dataset. Conversely, the minimum thrombus thickness ($t_{t,mim}$) was used in only 6.67% of the instances. Similar attribute uses are reported in Table 6 for classification problems (II) – (IV).

6. DISCUSSION

The purpose of this study was two-fold: (i) to assess the discrepancy between two methods for quantifying AAA diameter and wall thickness, and (ii) to derive a set of geometric indices that can classify an aneurysm as either electively repaired or emergently repaired based on a decision tree machine learning algorithm. To this end, we found that calculating D_{max} for Group 1 (electively repaired AAA) in planes orthogonal to the medial axis yielded diameters 2.48 ± 4.19 mm larger than those calculated in planes orthogonal to the aneurysm centerline. Likewise, D_{max} for Group 2 (emergently repaired AAA) was 3.99 ± 3.18 mm larger with respect to the medial axis than with respect to the centerline. These differences in aneurysm diameter were found to be statistically significant for both groups ($p < 0.05$). The *range* of diameter differences for Group 1 was 24.25 mm and 16.75 mm for Group 2. In addition, the average wall thicknesses for Group 1 calculated with both methods were different by 0.13 0.27 mm and this difference was significant ($p < 0.05$). For Group 2, the average wall thickness calculated with respect to the centerline was 0.18 0.18 mm higher than that calculated with respect to the medial axis, and this difference too was statistically significant ($p < 0.05$).

The work performed by Gharahi *et al.*[6] on 3 AAA showed that D_{max}, when calculated with respect to "axial and orthogonal planes", differ on average by 4 mm with the maximum difference being 15 mm. Novak and co-workers concluded that the median of the axial diameter (58.0 mm) was significantly higher ($p < 0.001$) than the median of the orthogonal diameter (54.5 mm).[17] A study conducted by Kontopodis and colleagues[9] reported a consistently higher axial measurement of D_{max} compared to the orthogonal measurement. A mean difference of 2.0 2.8 mm and a range of differences of 0 – 12.3 mm were obtained.

This over-estimation of maximum diameter could have resulted in 20% (12 of 60) patients undergoing AAA repair based on their size.

The regional distribution of wall thickness has been shown to affect aneurysm growth rate in finite element models[21] and is hypothesized to be a marker of rupture risk.[5] Conlisk *et al.*[1] concluded that upon inclusion of patient specific wall thickness, their rupture potential index increased by a factor of 2 in a study of 8 AAA. Wall thickness has also been known to affect mechanical wall stress and hence has the potential to influence rupture risk.[16] Thus, it is imperative to obtain accurate, non-invasive wall thickness measurements on an individual basis. Di Martino *et al.*[3] observed that ruptured aneurysm specimens had thicker walls than unruptured aneurysms. Our work corroborates these findings, which are independent of the axis used for the orthogonal planes.

In a classification study conducted by Lee *et al.*[13] with 190 patient specific AAA, the efficacy of surface curvatures was evaluated in classifying the AAA into unruptured and ruptured AAA. Their results indicate that the L2-norm of the Gaussian and Mean curvatures (*GLN* and *MLN*) yielded the highest classification accuracy (85.5%) using a k-nearest neighbors classification algorithm. The decision trees obtained in our study yielded *GLN* as the significant surface curvature index. Therefore, the present work supports the notion that surface curvature may also be used to classify an AAA as either electively or emergently repaired.

Our analysis of the four classification problems shows that the best average decision tree performance was achieved when only diameter-related indices calculated with respect to the AAA centerline are included in the classifier [i.e., classification problem (II)], as reflected by the highest values of average classification accuracy, and AUC. These average statistics were reported by using the decision tree classifier with 1000 different training sets (of 105 AAA each) and 1000 different testing sets (of 45 AAA each). However, the maximum accuracy for any of the iterations executed for all classification problems was found when all 16 diameter- and wall thickness-related indices were calculated with respect to the AAA centerline [i.e., classification problem (IV)], yielding a classification accuracy of 95.6%. While the average classification accuracy of problem (II) is only marginally higher than that of problems (I), (III) and (IV), the and AUC statistics showed differences that are more significant. Nevertheless, we cannot conclusively state that the inclusion of diameter-related indices calculated with respect to the AAA centerline are necessary to obtain an accurate decision tree. Since the majority of the 16 diameter- and wall thickness-related indices were statistically significant for Groups 1 and 2 depending on the axis used for their calculation, we recommend the use of planes orthogonal to the AAA centerline to derive such indices.

The decision trees built for all classification problems had the following in common: (i) the top three most important geometrics indices in the classifiers were, in order, *L*, *GLN*, and *S*; and (ii) the maximum aneurysm diameter was not an attribute used in any of the classifiers. Therefore, the AAA centerline length, the L2-norm of the Gaussian curvature, and the surface area of the AAA wall are the geometric measures that can best discriminate between an electively repaired and an emergently repaired AAA, based on these having the highest information gain in the application of the decision tree classifier. The use of geometric

indices in a clinical setting is advantageous because of their ease of interpretation by physicians in rupture risk assessment. Using decision tress yields threshold values for the indices that have the highest classification accuracy where tree branching takes place. This is an evident advantage of decision tress compared to other machine learning algorithms such as support vector machines, K-nearest neighbors, and Naïve-Bayes. The model trained by Shum *et al.*[24] had a classification accuracy of 86.6%; however, due to the skewed nature of their sample size, was relatively low (0.37). In the present work, an equal number of AAA were used for Groups 1 and 2, leading to a more robust classifier with an average in the range 0.59 0.68. This yields a machine learning classifier that can accurately discriminate AAA based on retrospectively acquired training data and assess rupture risk with a prospective testing dataset.

The present work is subject to some important limitations. As the algorithm used to calculate planes orthogonal to the centerline considers two consecutive points at a time, a plane is not found for the last point of the centerline. In addition, there was variability in the image slice spacing (0.25 to 3 mm) of the dataset. This led to variability in the number of binary masks resulting from the image segmentation step and the need for interpolation and smoothing to be performed in those cases with large slice spacing.

There is suspected intra-observer variability in the segmentation of the clinical images, although its effect on the classifiers was not quantified. There is also variability in the pixel size of the images. In this regard, the wall thickness calculation is limited by the pixel size and the intensity gradient across the vascular wall; the larger the pixels, the less precise the wall thickness prediction. The use of mathematical formulations for the quantification of 47 geometric indices *a priori* is another limiting aspect of our geometry quantification approach. There could be shape measures important for differentiation amongst individual AAA that are not taken into account by our methodology and could be predicted by using techniques that quantify cylindrical harmonics. Moreover, the classification analyses were limited to the use of measures of geometry. These can be improved in a future study by including additional measures such as wall mechanics and/or tissue composition metrics (such as those obtained from immunohistochemistry). Wall mechanics is dependent on the choice of the constitutive material model used to predict the arterial mechanical behavior. In addition, tissue composition is subject to the availability of AAA wall specimens for subsequent histological analysis. Therefore, the inclusion of non-geometric measures in a classification analysis may be limited by the accessibility to individual clinical data.

Supplementary Material

Refer to Web version on PubMed Central for supplementary material.

7. ACKNOWLEDGMENTS

8. REFERENCES

1. Conlisk N, Geers AJ, McBride OM, Newby DE and Hoskins PR Patientspecific modelling of abdominal aortic aneurysms: The influence of wall thickness on predicted clinical outcomes. Medical Engineering & Physics 38: 526–537, 2016. [PubMed: 27056256]

2. Darling RC, Messina CR, Brewster DC and Ottinger LW Autopsy study of unoperated abdominal aortic aneurysms. The case for early resection. Circulation 56: II161–164, 1977.

3. Di Martino ES, Bohra A, Geest JPV, Gupta N, Makaroun MS and Vorp DA Biomechanical properties of ruptured versus electively repaired abdominal aortic aneurysm wall tissue. Journal of Vascular Surgery 43: 570–576, 2006. [PubMed: 16520175]

4. Doyle BJ, Callanan A, Burke PE, Grace PA, Walsh MT, Vorp DA and McGloughlin TM Vessel asymmetry as an additional diagnostic tool in the assessment of abdominal aortic aneurysms. Journal of Vascular Surgery 49: 443–454, 2009. [PubMed: 19028061]

5. Gasser TC, Auer M, Labruto F, Swedenborg J and Roy J Biomechanical rupture risk assessment of abdominal aortic aneurysms: model complexity versus predictability of finite element simulations. European Journal of Vascular and Endovascular Surgery 40: 176–185, 2010. [PubMed: 20447844]

6. Gharahi H, Zambrano B, Lim C, Choi J, Lee W and Baek S On growth measurements of abdominal aortic aneurysms using maximally inscribed spheres. Medical Engineering & Physics 37: 683–691, 2015. [PubMed: 26004506]

7. Golledge J, Norman PE, Murphy MP and Dalman RL Challenges and opportunities in limiting abdominal aortic aneurysm growth. Journal of Vascular Surgery 65: 225–233, 2017. [PubMed: 27641464]

8. Healey CT, Neilson M, Clark D, Schanzer A and Robinson W Predicting mortality of ruptured abdominal aortic aneurysms in the era of endovascular repair. Annals of Vascular Surgery 38: 59–63, 2017. [PubMed: 27794443]

9. Kontopodis N, Metaxa E, Gionis M, Papaharilaou Y and Ioannou CV Discrepancies in determination of abdominal aortic aneurysms maximum diameter and growth rate, using axial and orthogonal computed tomography measurements. European Journal of Radiology 82: 1398–1403, 2013. [PubMed: 23727377]

10. Kontopodis N, Pantidis D, Dedes A, Daskalakis N and Ioannou CV The –not so– solid 5.5 cm threshold for abdominal aortic aneurysm repair: Facts, misinterpretations, and future directions. Frontiers in Surgery 3: 2016.

11. Kuhn M, Weston S, Coulter N and Quinlan R C50: C5.0 decision trees and rule-based models. R package version 0.1. 0–21, *URL* https://cran.rproject.org/web/packages/C50/C50.pdf

12. Lederle FA, Wilson SE, Johnson GR, Reinke DB, Littooy FN, Acher CW, Ballard DJ, Messina LM, Gordon IL and Chute EP Immediate repair compared with surveillance of small abdominal aortic aneurysms. New England Journal of Medicine 346: 1437–1444, 2002. [PubMed: 12000813]

13. Lee K, Zhu J, Shum J, Zhang Y, Muluk SC, Chandra A, Eskandari MK and Finol EA Surface curvature as a classifier of abdominal aortic aneurysms: a comparative analysis. Annals of Biomedical Engineering 41: 562–576, 2013. [PubMed: 23180028]

14. Manning BJ, Kristmundsson T, Sonesson B and Resch T Abdominal aortic aneurysm diameter: a comparison of ultrasound measurements with those from standard and three-dimensional computed tomography reconstruction. Journal of Vascular Surgery 50: 263–268, 2009. [PubMed: 19631858]

15. Martufi G, Di Martino ES, Amon CH, Muluk SC and Finol EA Threedimensional geometrical characterization of abdominal aortic aneurysms: imagebased wall thickness distribution. Journal of Biomechanical Engineering 131: 061015, 2009. [PubMed: 19449969]

16. Mower WR, Baraff LJ and Sneyd J Stress distributions in vascular aneurysms: factors affecting risk of aneurysm rupture. Journal of Surgical Research 55: 155–161, 1993. [PubMed: 8412094]

17. Novak K, Polzer S, Krivka T, Vlachovsky R, Staffa R, Kubicek L, Lambert L and Bursa J Correlation between transversal and orthogonal maximal diameters of abdominal aortic aneurysms and alternative rupture risk predictors. Computers in Biology and Medicine 83: 151–156, 2017. [PubMed: 28282590]

18. Pappu S, Dardik A, Tagare H and Gusberg RJ Beyond fusiform and saccular: a novel quantitative tortuosity index may help classify aneurysm shape and predict aneurysm rupture potential. Annals of Vascular Surgery 22: 88–97, 2008. [PubMed: 18023556]

19. Raghavan ML, Kratzberg J, de Tolosa EMC, Hanaoka MM, Walker P and da Silva ES Regional distribution of wall thickness and failure properties of human abdominal aortic aneurysm. Journal of Biomechanics 39: 3010–3016, 2006. [PubMed: 16337949]

20. Raut SS, Liu P and Finol EA An approach for patient-specific multi-domain vascular mesh generation featuring spatially varying wall thickness modeling. Journal of Biomechanics 48: 1972–1981, 2015. [PubMed: 25976018]

21. Shang EK, Nathan DP, Woo EY, Fairman RM, Wang GJ, Gorman RC, Gorman JH and Jackson BM Local wall thickness in finite element models improves prediction of abdominal aortic aneurysm growth. Journal of Vascular Surgery 61: 217–223, 2015. [PubMed: 24095043]

22. Shelmerdine S, Barber J and George C Applications of Laplace's law in clinical medicine: a radiological pictorial review. Br J Hosp Med 74: 451–456, 2013.

23. Shum J, DiMartino ES, Goldhammer A, Goldman DH, Acker LC, Patel G, Ng JH, Martufi G and Finol EA Semiautomatic vessel wall detection and quantification of wall thickness in computed tomography images of human abdominal aortic aneurysms. Medical Physics 37: 638–648, 2010. [PubMed: 20229873]

24. Shum J, Martufi G, Di Martino E, Washington CB, Grisafi J, Muluk SC and Finol EA Quantitative assessment of abdominal aortic aneurysm geometry. Annals of Biomedical Engineering 39: 277–286, 2011. [PubMed: 20890661]

25. Shum J, Xu A, Chatnuntawech I and Finol EA A framework for the automatic generation of surface topologies for abdominal aortic aneurysm models. Annals of Biomedical Engineering 39: 249–259, 2011. [PubMed: 20853025]

26. Szilagyi DE, Smith RF, DeRusso FJ, Elliott J. h. P. and Sherrin FW Contribution of abdominal aortic aneurysmectomy to prolongation of life. Annals of Surgery 164: 678, 1966. [PubMed: 5924789]

27. Tang A, Kauffmann C, Tremblay-Paquet S, Elkouri S, Steinmetz O, MorinRoy F, Cloutier-Gill L and Soulez G Morphologic evaluation of ruptured and symptomatic abdominal aortic aneurysm by three-dimensional modeling. Journal of Vascular Surgery 59: 894–902. e893, 2014. [PubMed: 24439318]

28. Vorp DA Biomechanics of abdominal aortic aneurysm. Journal of Biomechanics 40: 1887–1902, 2007. [PubMed: 17254589]

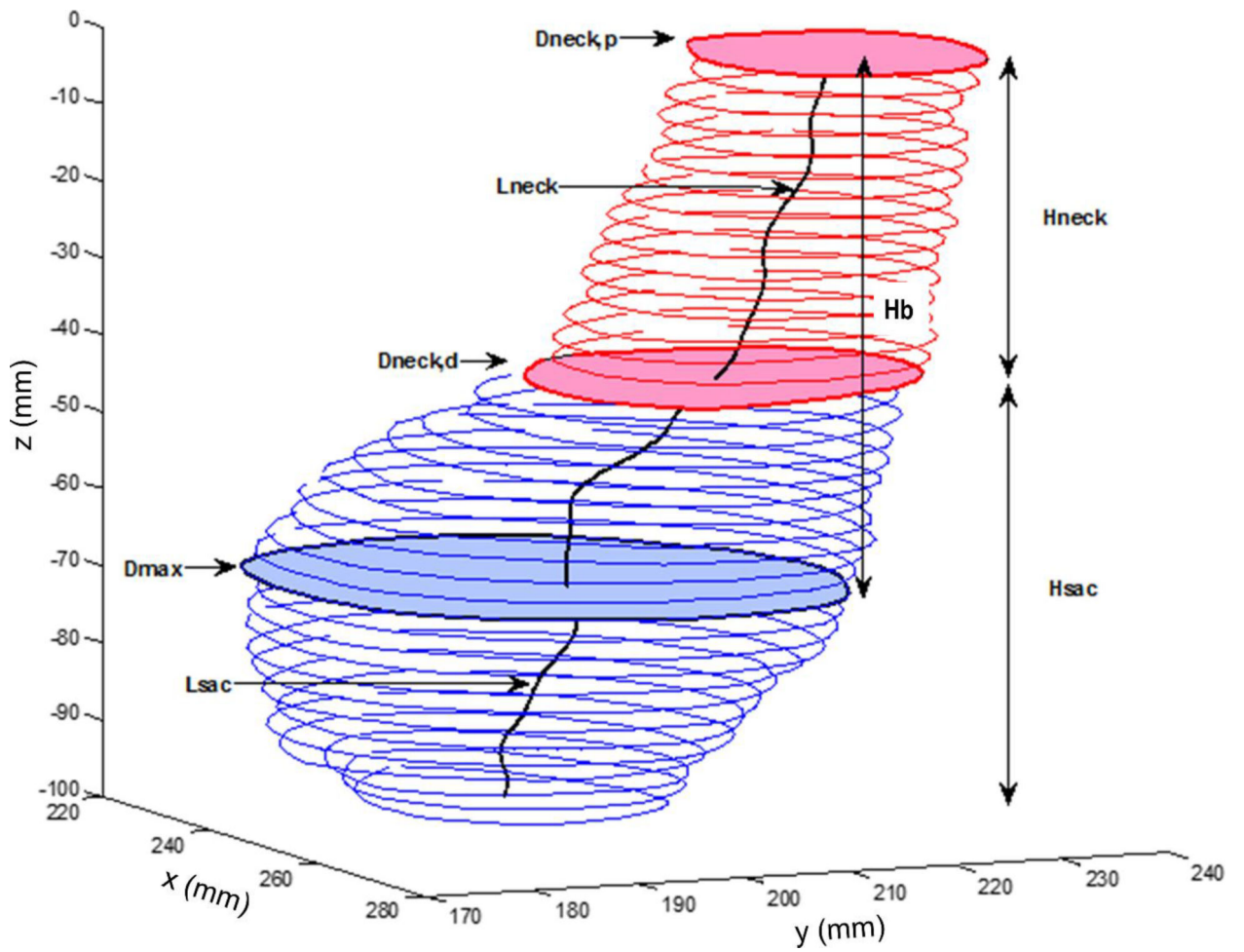**Figure 1:**
Schematic representation of 1-D geometric indices calculated using planes orthogonal to the medial axis (reproduced from [10]).
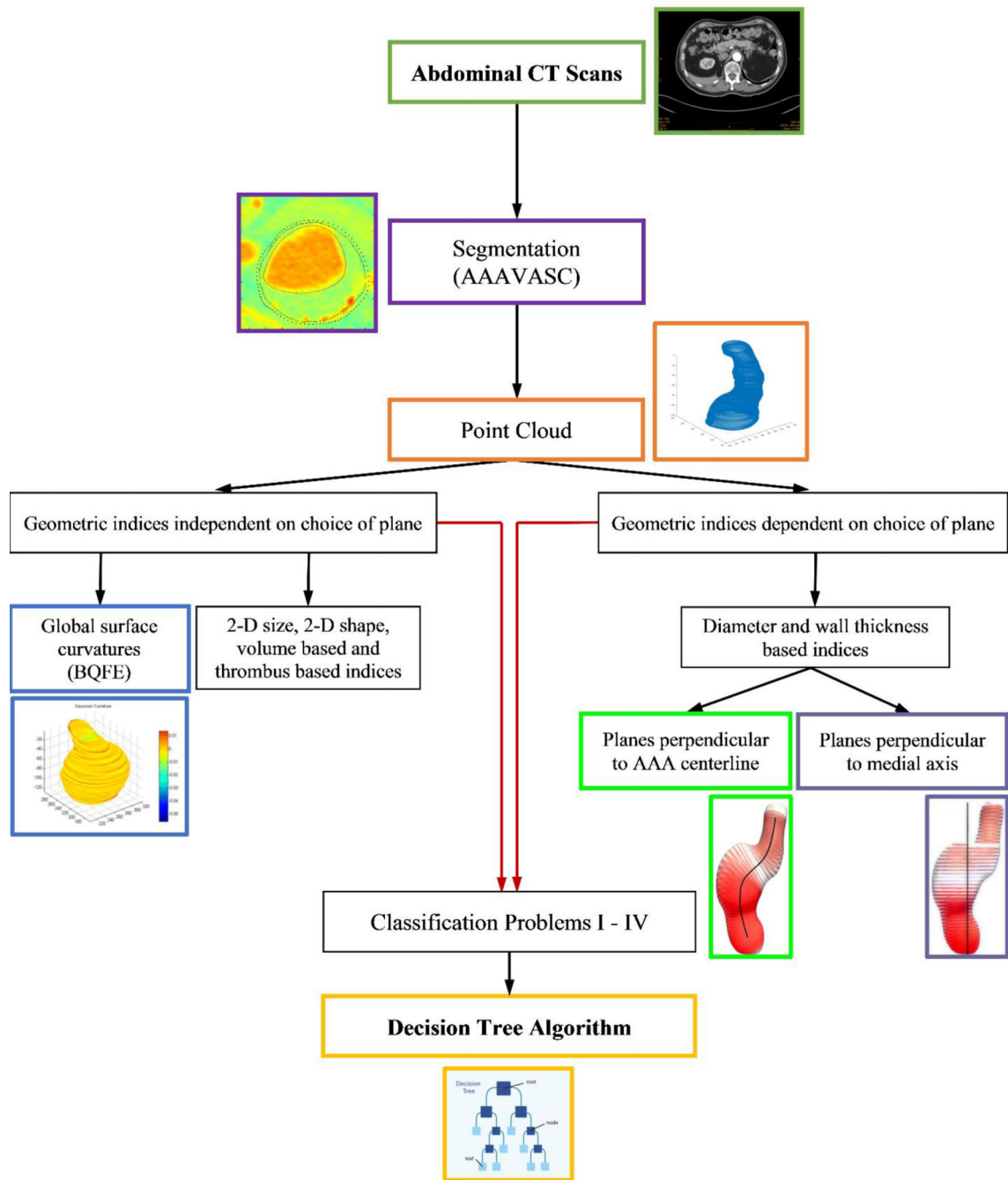
Figure 2:
Schematic of the workflow followed in segmenting the clinical images, meshing the AAA models, evaluating the geometric indices, and performing statistical and decision tree learning analyses. Insets reproduced from [9] and [23].
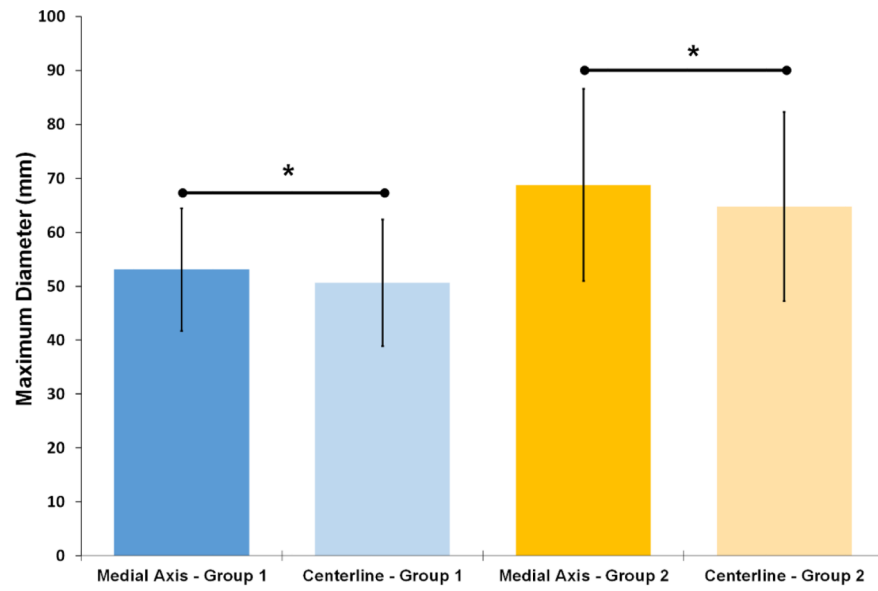
(a)
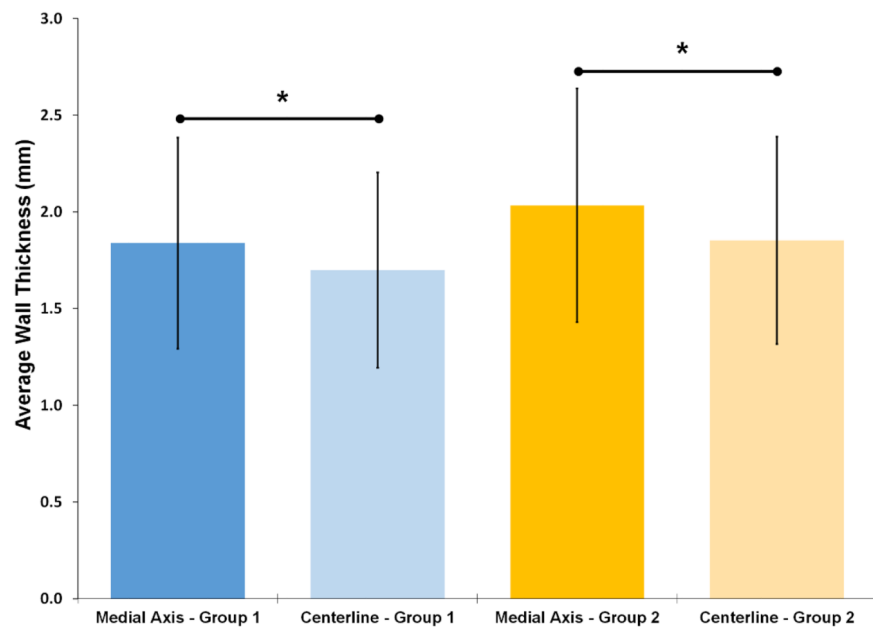
(b)

Figure 3:

Comparison of the mean (a) D_{max} and (b) $t_{w,ave}$ calculated relative to the medial axis and centerline for both AAA groups. The differences among the groups are statistically significant ($p < 0.05$).

Figure 4:
Exemplary C5.0 decision tree model obtained from the application of the machine learning algorithm. This model is based on the entire dataset for classification problem (I), indicating that the centerline length of the AAA (L) is the feature with the highest information gain and the root of the tree. The correctly classified and misclassified instances at a particular node are indicated by the (/) sign.

Table 1:
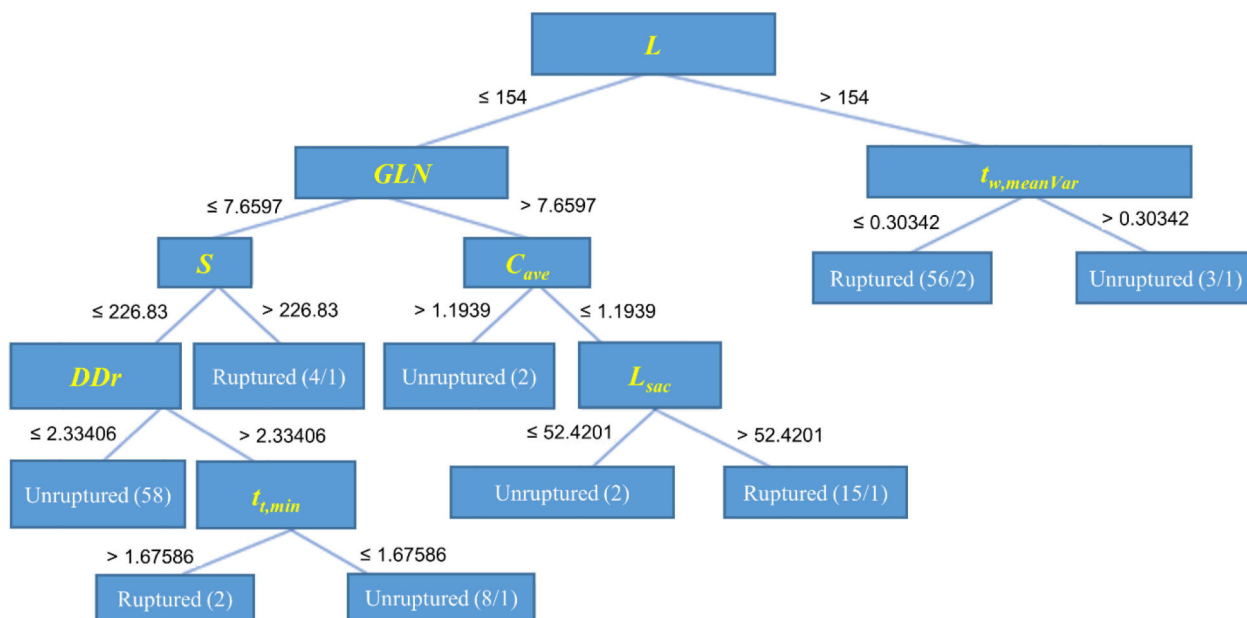
P-values obtained from paired t-tests with the 16 indices dependent on the AAA centerline signifying difference of the means when compared to indices calculated relative to the medial axis ($p < 0.05$ was deemed to represent statistical significance).

Geometric Index	Group 1	Group 2
D_{max}	< 0.0001	< 0.0001
dc	0.256	0.734
DDr	0.002	0.028
β	0.378	0.435
$t_{w,ave}$	< 0.0001	< 0.0001
$t_{w,max}$	< 0.0001	< 0.0001
$t_{w,min}$	< 0.0001	< 0.0001
$t_{w,Dmax}$	< 0.0001	< 0.0001
$t_{w,mode}$	< 0.0001	< 0.0001
$t_{w,median}$	< 0.0001	< 0.0001
$t_{w,minVar}$	0.351	0.365
$t_{w,MaxVar}$	0.0166	0.050
$t_{w,meanVar}$	< 0.0001	< 0.0001
$t_{w,medianVar}$	< 0.0001	< 0.0001
$PercentAbove$	0.351	< 0.0001
$PercentBelow$	< 0.0001	0.356

Table 2:

The 31 geometric indices calculated for Group 1 (electively repaired AAA) and Group 2 (emergently repaired AAA).

Geometric Index	Group 1 (n = 75)		Group 2 (n = 75)	
	Mean	Std. Deviation	Mean	Std. Deviation
$D_{neck,p}$	29.147	8.959	32.019	8.709
$D_{neck,d}$	27.722	15.894	28.440	17.858
H	100.607	18.434	114.231	24.743
L	26.140	19.234	21.173	19.897
H_{neck}	74.467	21.843	93.058	32.037
L_{neck}	127.623	21.513	184.568	49.424
H_{sac}	44.379	34.061	36.585	40.401
L_{sac}	83.244	32.556	147.985	49.877
H_b	59.933	18.370	78.840	37.040
DHr	0.572	0.369	0.657	0.567
Hr	0.264	0.203	0.196	0.183
BL	0.631	0.405	0.718	0.360
β	1.276	0.457	1.677	0.972
C_{ave}	1.115	0.075	1.139	0.060
C_{min}	1.492	0.430	1.783	0.412
C_{max}	1.025	0.026	1.024	0.016
$t_{t,ave}$	6.932	4.019	9.696	5.957
$t_{t,max}$	19.948	9.965	27.853	14.679
$t_{t,min}$	1.558	0.138	1.511	0.192
$t_{t,minLoc}$	0.451	0.344	0.620	0.510
$t_{t,maxLoc}$	0.674	0.492	0.810	0.493
V	190.905	209.611	320.148	211.493
S	163.619	55.443	237.939	97.750
V_{ILT}	67.311	59.888	143.933	122.456
	0.358	0.196	0.419	0.194
NFI	1.090	0.169	1.089	0.110
IPR	5.336	1.073	5.431	0.381
GAA	$8.096 \ 10^{-5}$	$8.456 \ 10^{-5}$	$8.813 \ 10^{-5}$	$4.046 \ 10^{-5}$
MAA	0.024	0.005	0.020	0.008
GLN	6.063	2.151	18.340	51.506
MLN	0.640	0.176	1.333	1.450

Table 3:

The 16 diameter- and wall thickness-related indices calculated with respect to the medial axis and AAA centerline for Group 1. The statistical significance of the differences is assessed in Table 1.

Geometric Index	Group 1 (n = 75)			
	Medial axis		Centerline	
	Mean	Standard Deviation	Mean	Standard Deviation
D_{max}	53.084	11.368	50.600	11.763
dc	5.563	4.750	5.054	3.969
DDr	1.900	0.482	1.809	0.492
β	0.902	0.071	0.999	0.939
$t_{w,ave}$	1.838	0.547	1.699	0.504
$t_{w,max}$	3.942	1.719	3.158	1.126
$t_{w,min}$	0.629	0.234	0.486	0.226
$t_{w,Dmax}$	1.829	0.602	1.655	0.529
$t_{w,mode}$	1.721	0.652	0.524	0.227
$t_{w,median}$	1.822	0.583	1.704	0.534
$t_{w,minVar}$	0.046	0.049	0.053	0.063
$t_{w,MaxVar}$	0.672	1.482	1.122	0.771
$t_{w,meanVar}$	0.173	0.181	0.417	0.292
$t_{w,medianVar}$	0.133	0.142	0.331	0.287
$PercentAbove$	42.874	8.907	49.049	9.121
$PercentBelow$	57.127	8.907	49.625	4.2185

Table 4:

The 16 diameter- and wall thickness-related indices calculated with respect to the medial axis and AAA centerline for Group 2. The statistical significance of the differences is assessed in Table 1.

Geometric Index	Group 2 (n = 75)			
	Medial axis		Centerline	
	Mean	Standard Deviation	Mean	Standard Deviation
D_{max}	68.777	17.825	64.600	11.763
dc	7.362	6.025	7.218	5.473
DDr	2.222	0.589	2.130	0.660
β	0.897	0.074	0.887	0.115
$t_{w,ave}$	2.034	0.603	1.852	0.537
$t_{w,max}$	4.973	2.511	3.963	1.362
$t_{w,min}$	0.645	0.318	0.403	0.369
$t_{w,Dmax}$	2.161	0.801	1.804	0.566
$t_{w,mode}$	1.904	0.632	0.474	0.273
$t_{w,median}$	2.005	0.624	1.829	0.570
$t_{w,minVar}$	0.051	0.031	0.068	0.159
$t_{w,MaxVar}$	0.923	1.769	1.346	0.731
$t_{w,meanVar}$	0.177	0.113	0.534	0.312
$t_{w,medianVar}$	0.138	0.088	0.448	0.345
$PercentAbove$	43.713	7.248	49.255	4.819
$PercentBelow$	55.839	7.084	50.375	4.517

Table 5:

C5.0 decision tree model statistics for all classification problems; averaged over 1000 iterations and the maximum of all iterations.

Classification Problem	Classification accuracy (%) – average / maximum	Kappa statistic ( ) – average / maximum	Area under ROC curve (AUC) – average / maximum
(I)	80.6 ± 6.0	0.61 ± 0.12	0.81 ± 0.06
	95.5	0.91	0.96
(II)	81.0 ± 5.7	0.68 ± 0.11	0.84 ± 0.06
	95.5	0.91	0.95
(III)	80.1 ± 5.2	0.59 ± 0.10	0.82 ± 0.05
	93.3	0.87	0.94
(IV)	80.2 ± 5.8	0.60 ± 0.12	0.80 ± 0.06
	95.6	0.91	0.96

Table 6:

Relative importance of attributes in the C5.0 decision tree models for classification problems (I) – (IV). The top three most important geometrics indices in the classifiers were, in order, L, GLN, and S.

Classification Problem (I)		Classification Problem (II)	
Geometric Index (attribute)	**Frequency of Inclusion (%)**	**Geometric Index (attribute)**	**Frequency of Inclusion (%)**
L	100.00	L	100.00
GLN	60.67	GLN	60.67
S	48.00	S	48.00
DDr	45.33	DDr	45.33
$t_{w,meanVar}$	39.33	$t_{w,meanVar}$	39.33
C_{ave}	12.67	C_{ave}	12.67
L_{sac}	11.33	L_{sac}	11.33
$t_{t,min}$	6.67	$t_{t,min}$	6.67
Classification Problem (III)		**Classification Problem (IV)**	
Geometric Index (attribute)	**Frequency of Inclusion (%)**	**Geometric Index (attribute)**	**Frequency of Inclusion (%)**
L	100.00	L	100.00
GLN	60.67	GLN	60.67
S	48.00	S	48.00
$t_{t,min}$	46.00	DDr	45.33
DDr	45.33	C_{ave}	12.67
C_{ave}	12.67	L_{sac}	11.33
L_{sac}	11.33	$t_{w,min}$	5.33